Electrochemically Assisted Sol−Gel Process for the Synthesis of Polysiloxane Films Incorporating Phenothiazine Dyes Analogous to Methylene Blue. Structure and Ion-Transport Properties of the Films via Spectroscopic and Electrochemical Characterization

Nicholas Leventis* and Muguo Chen

Department of Chemistry, The University of Missouri at Rolla, Rolla, Missouri 65409-0249

Received April 29, 1997. Revised Manuscript Received July 25, 1997[⊗]

A sol−gel process is directed toward an electrode surface via electrochemical manipulation of the solubility of trimethoxysilyl group-modified methylene blue in an aqueous environment. The process lasts for 2−3 h and results in electrode derivatization with a polysiloxane network incorporating methylene blue. Cross-linking (curing) is completed by drying the films at room temperature for 2 days. The concentration of the phenothiazine moieties in the resulting xero films was calculated at ∼3.9 M, and the film density at ∼2.6 g/cm^3. The average distance between phenothiazine moieties is <5 Å allowing interactions between their π-systems. The narrow pores between monomer units restrict movement of hydrated charge-compensating ions, so that the redox switching of the films depends upon the chemical identity of both the cation and anion of the supporting electrolyte. The films retain the electrochromic and electrocatalytic properties of the parent dye; for example, gold electrodes derivatized with the film mediate reduction of cytochrome *c* at potentials close to its standard electrochemical potential.

Introduction

The sol−gel process provides materials with composition identical with that of high temperature glasses and ceramics via room-temperature polymerization of metal and semimetal hydroxides or hydrolysis and polymerization of their ethers (particularly alkoxides) or esters.[1] Because of the room-temperature conditions the sol−gel process is convenient for preparation of glasses doped with temperature sensitive substances such as laser dyes, proteins, etc., which is, of course, impossible with the high-temperature melts of regular glass manufacturing.[2] As a result, various novel materials have appeared recently and are suitable either for pure optical applications (light guides, dye lasers, optical memories, nonlinear optics, etc.) or for applications that involve interaction of the dopant with external molecules (e.g., electrochemical and electrobiochemical sensors, electrochromics, batteries, sensors based on photocatalysis, etc.).[3]

The two most frequent concerns with respect to doped xerogels (the final glass or ceramic-like material of a sol−gel process) are leaching of the dopant, and particularly for electrochemical (but also for optical sensor) applications, the response time, which is related to the time required to access the redox-active material entrapped in the bulk of the xerogel.[4] Covalent bonding by copolymerization of modified dopants [usually with $-Si(OCH_3)_3$ groups] with sol−gel precursors comprises an efficient solution to the leaching problem,[4] while in principle films of sol−gel materials should possess the best response time because of the short diffusion path.

At this point we reasoned that for electrochemical applications if an alkoxysilane-modified redox-active dopant could be polymerized by itself, both the leaching problem would be solved and the best access time for a given amount of the dopant could be achieved, as that amount would be accommodated by the thinnest film possible with the closest proximity between the redox-active units for the fastest site-to-site electron hoping to take place. Since organic dyes are attractive as dopants,[2,3] we reasoned further that once a redox-active dye is modified with $-Si(OCH_3)_3$ groups, a sol−gel process could possibly be directed onto an electrode if the product of hydrolysis and partial oligomerization of the modified dye (sol) could precipitate on the surface of that electrode by electrochemical manipulation of its solubility. Even though electrodeposition of nanostructured films is an area actively pursued,[5] to our knowledge that powerful method has not been applied to sol−gel materials incorporating dyes despite its potential technological significance.

* Address correspondence to this author. E-mail: leventis@umr.edu tel.: (573) 341-4391.

[⊗] Abstract published in *Advance ACS Abstracts,* October 1, 1997.

(1) (a) Hench, L. L.; West, J. K. *Chem. Rev. (Washington, D.C.)* **1990**, *90*, 33. (b) Avnir, D. *Acc. Chem. Res.* **1995**, *28*, 328. (c) Brinker, C. J.; Scherer, G. W. *Sol−Gel Science. The Physics and Chemistry of Sol−Gel Processes*; Academic Press: New York, 1990.

(2) (a) Avnir D.; Levy, D.; Reisfeld, R. *J. Phys. Chem.* **1984**, *88*, 5956. (b) Severin-Vantilt, M. M. E.; Oomen, E. W. J. L. *J. Non-Cryst. Sci.* **1993**, *159*, 38.

(3) Aharonson, N.; et al. *Mater. Res. Soc. Symp.* **1994**, *346*, 519.

(4) (a) Lev, O.; Tsionsky, M.; Rabinovich, L.; Glezer, V.; Sampath, S.; Pankratov, I.; Gun, J. *Anal. Chem.* **1995**, *67*, 22A. (b) Dave, B. C.; Dunn, B.; Selverstone Valentine, J.; Zink, J. I. *Anal. Chem.* **1994**, *66*, 1120A.

(5) (a) Switzer, J. A.; Hung, C.-J.; Breyfogle, B. E.; Shumsky, M. G.; Van Leeuwen, R.; Golden, T. D. *Science* **1994**, *264*, 1573. (b) Curtis, C. L.; Ritchie, J. E.; Sailor, M. J. *Science* **1993**, *262*, 2014. (c) Moran, M.; Casado, C. M.; Cuadrado, I.; Losada, J. *Organometallics* **1993**, *12*, 4327. (d) Switzer, J. A.; Shane, M. J.; Phillips, R. J. *Science* **1990**, *247*, 444.

S0897-4756(97)00261-5 CCC: $14.00

To explore the feasibility of our hypothesis, we chose methylene blue (MB) as the model dye,[6] not only because of its demonstrated utility in electrocatalysis,[7] electrochromics,[8] and photoelectrochemical imaging,[9] but also because its solubility is known to change upon reduction in aqueous solutions, so that at pH = 7.9 leucomethylene blue (LMB) films of up to ca. 50 monolayers thick are formed reversibly on Au and Pt electrodes.[10] Furthermore, the spectroscopic and electrochemical properties of MB are well understood (eqs 1 and 2)[11] and would comprise an excellent point of reference for the new material.

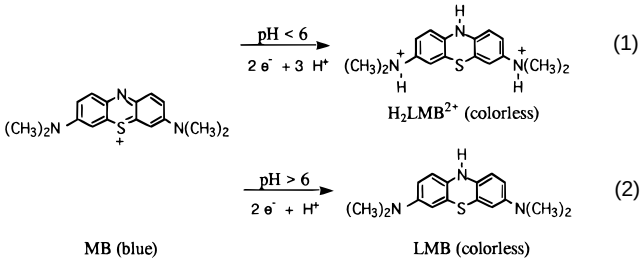

Along these lines, the alkoxysilane-modified phenothiazine dye **I** was designed to retain the substitution pattern of the MB chromophore and could be prepared via hydrosylilation[12] of **II**, whose synthesis was described elsewhere.[13]

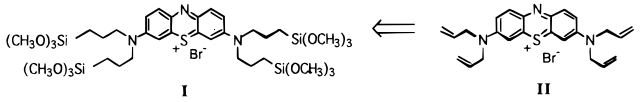

Experimental Section

All starting materials for synthesis, deuterated solvents, and the salts used as electrolytes were of the highest purity available from Aldrich. Horse heart cytochrome *c* (MW = 12 384) was purchased from Sigma. Water used as solvent in the electrochemical experiments was HPLC grade obtained from Fisher Scientific.

For materials characterization, ^{1}H NMR spectra were obtained at Washington University in St. Louis with a Unity-Plus 500 NMR spectrometer of Varian Corporation. Elemental analysis was performed by Oneida Research Services, Inc. (Whiteboro, NY).

Synthesis of 3,7-bis[di-2-propenylamino]phenothiazin-5-ium bromide (**II**) has been described elsewhere.[13]

Synthesis of 3,7-Bis[bis(trimethoxysilyl-3-propyl)-amino]phenothiazin-5-ium Bromide (I): II (0.45 g, 0.96 mmol) was dissolved in anhydrous methanol (50 mL) and the solution was placed in a round-bottom flask fitted with a condenser and drying tube, and heated to 65 °C with an oil bath. To the warm solution, 11.1 mg of H_2PtCl_6 was added dissolved in ~8 drops of isopropyl alcohol. After 10 min $HSi(OCH_3)_3$ (2.5 mL, 19.6 mmol) was added in the round-bottom flask, and the solution quickly turned (within 3 min) from blue to green and eventually to brown. At that point the oil bath was removed, the flask was covered with an aluminum foil, and the solution was stirred at room temperature for 36 h. Two to four hours after the oil bath was removed the solution started turning back to blue. At the end of the stirring period, the solution was dark blue again; then most of the solvent was removed with a rotary evaporator, and the concentrated solution (5−10 mL) was added dropwise to ether (200 mL). The product precipitated out, was collected and recrystallized once with methanol/ether. Received 0.32 g (35% yield). It has been found that **I** is most stable against polymerization if it is kept refrigerated as a methanolic solution. ^{1}H NMR (CD_3OD, 500 MHz) δ 0.76 (t, J = 8.3 Hz, 8H), 1.06 (t, J = 7.3 Hz, 8H), 1.78 (m, 8H), 3.34 (s, 36 H), 7.10 (d, J_m = 2.44 Hz, 2H), 7.22 (dd, J_m = 2.44 Hz, J_o = 9.28 Hz, 2H), 7.93 (d, J_o = 9.28 Hz, 2 H); IR (KBr) 904 (m), 1131 (m), 1228 (m), 1327 (m), 1392 (s), 1489 (m), 1604 (s), 2900−3200 (m) cm^{-1}; elemental analysis: Calcd for $C_{36}H_{66}N_3O_{12}Si_4SBr$: C, 45.17; H, 6.95; N, 4.39. Found: C, 45.95; H, 6.89; N, 4.43.

Gold and platinum disk electrodes and Ag/AgCl reference electrodes were purchased from Bioanalytical systems (West Lafayette, IN). ITO-coated glass (≤8 Ω/□) was purchased from Donnelly Applied Films Corp. (Boulder, CO). Gold and platinum foil electrodes were cleaned with H_2O_2/H_2SO_4 (1:4 v/v); gold and platinum disk electrodes were polished using successively 6, 3, and 1 μm diamond paste on DR-Nap polishing cloth (all from Struers, Westlake, OH). ITO-coated glass was cleaned with Micro cleaning solution. ITO-coated glass was patterned photolithographically by first protecting the areas where ITO must remain with a layer (1.45 μm thick) of positive photoresist (Shipley SPR 700−1.0 μm, first span at 1500 rpm for 30 s, then soft baked at 90 °C for 30 min in a convection oven, then exposed through a mask for 50 s to UV light (2.44 mW/cm^2 of the *i*-line of an Optical Associates Inc. high-resolution aligner, Model J500/VIS), developed for 1 min with Shipley MF-321 positive photoresist developer, and finally hard baked with a hot plate at 140 °C for 1 min). ITO was etched off the unprotected areas by sonication in a 6 M aq HCl, 0.2 M $FeCl_3$ etching solution for 12 min.[14]

Au, Pt, and ITO electrodes were derivatized with films of **I** by cycling their potential at 50 mV/s through the reduction wave of **I** for 2−3 h in phosphate buffer (μ = 0.2, pH = 7.4) containing 5% CH_3OH and 2−3 mM of **I**. Polymerization and cross-linking is completed by drying the blue electrodes for 2 days in air at room temperature. Electrode coverage was calculated with slow cyclic voltammetry (5 mV/s) at about neutral pH in a KCl-based electrolyte.

Electronic absorption spectra were obtained with a Beckman Model 35 UV−vis spectrophotometer. For dilute solutions we used typical UV cuvettes, while for concentrated solutions we constructed special cells using two borosilicate glass microscope slides for each cell, separated along two edges with two glass spacers made of cover glass slides (150 μm thick) purchased from Fisher Scientific. The thin glass spacers were glued in place with clear epoxy (from The Dexter Corp., part no. 0151), and the final thickness of the cell was confirmed using a micrometer (5 μm resolution). The cells were filled by capillary action.

Infrared spectra were obtained with a Nicolet Magna IR spectrometer, Model 750. For grazing angle infrared spectra films were deposited on Cr/Au-coated glass slides, which subsequently were fitted into a special attachment obtained from Harrick Scientific Corp. (Ossining, NY).

(6) (a) *The Chemistry and Application of Dyes*; Waring, D. R., Hallas, G., Eds.; Plenum Press: New York, 1990. (b) Gordon, P. F.; Gregory, P. Non-textile Uses of Dyes. In *Critical Reports on Applied Chemistry; Developments in the Chemistry and Technology of Dyes*; Griffiths, J., Ed.; Blackwell: Oxford, 1984; Vol. 7, p 66.

(7) (a) Jiannong, Y.; Baldwin, R. P. *Anal. Chem.* **1988**, *60*, 2263. (b) Shihua, S.; Shaojun, D. *Bioelectrochem. Bioenerg.* **1988**, *19*, 337. (c) Fultz, M. L.; Durst, R. A. *Anal. Chim. Acta* **1981**, *140*, 1. (d) Brunori, M.; Saggese, U.; Rotilio, G.; Antonini, E.; Wyman, J. *Biochemistry* **1971**, *10*, 1604.

(8) (a) Byker, H. J. European Paten Application, No. 0,240,226, 1987. (b) Kuwabata, S.; Mitsui, K.; Yoneyama, H. *J. Electroanal. Chem.* **1990**, *281*, 97.

(9) Kuwabata, S.; Mitsui, K.; Yoneyama, H. *J. Electrochem. Soc.* **1992**, *139*, 1824.

(10) (a) Svetlicic, V.; Zutic, V.; Clavilier, J.; Chevalet, J. *J. Electroanal. Chem.* **1985**, *195*, 307. (b) Zutic, V.; Svetlicic, V.; Clavilier, J.; Chevalet, J. *J. Electroanal. Chem.* **1987**, *219*, 183.

(11) (a) Koryta, J. *Ions, Electrodes and Membranes*, 2nd ed.; Wiley: New York, 1991; p 89. (b) *Indicators*; Bishop, E., Ed.; Pergamon Press: New York, 1972.

(12) Speir, J. L. *Adv. Organomet. Chem.* **1979**, *17*, 407.

(13) Leventis, N.; Chen, M.; Sotiriou-Leventis, C. *Tetrahedron* **1997**, *53*, 10083.

(14) Van Den Meerakker, J. E. A. M.; Baarslag, P. C.; Scholten, M. *J. Electrochem. Soc.* **1995**, *142*, 2321.

Scheme 1. Synthesis of I

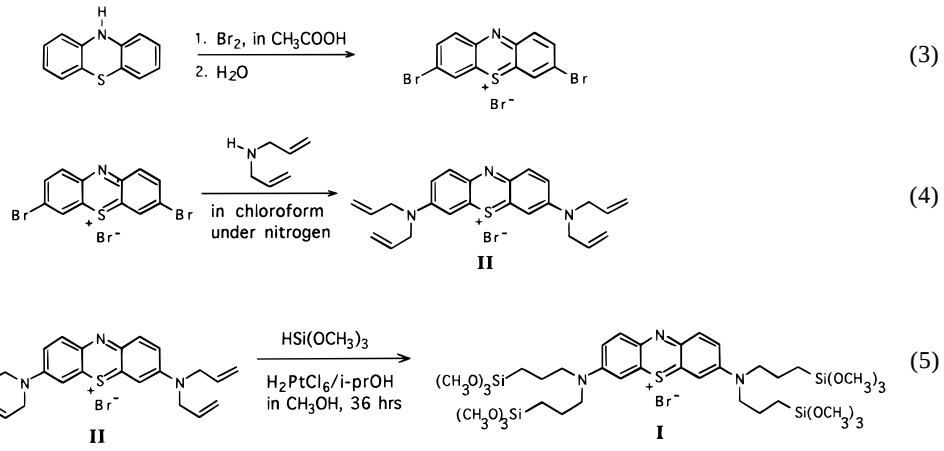

XPS spectra were obtained using a Physical Electronics Model 548 ESCA/Auger spectrometer. SEM pictures were obtained with a JEOL JSM-7330A scanning electron microscope. Film thickness measurements were carried out using a Dektak IIA profilometer.

All electrochemical experiments were carried out with either a PINE Instruments AFRDE5 bipotentiostat or an EG&G PAR 263A potentiostat. Cyclic voltammograms were recorded with a Kipp & Zonen *X,Y,Y′,T* recorder. All solutions were degassed with argon and kept under an argon blanket. For potential step chronoamperometric experiments, we used films deposited on Cr/Au- and Cr/Pt-coated microscope glass slides of known area, and data were collected with a Tektronics TDS 410A digitizing oscilloscope, stored on a disk, and plotted with a Macintosh computer. Quartz crystal microbalance data were collected with a Seiko EG&G QCA917 quartz crystal analyzer, and films which were electroplated directly onto quartz/gold oscillator/electrodes purchased from EG&G.

Molecular modeling was done using the Chem3D software package on a Macintosh computer.

Results and Discussion

Synthesis, Spectroscopy, and Electrochemical Characterization of Methylene Blue Analogue, I. The synthesis of **I** is summarized in Scheme 1. **II** was synthesized from phenothiazine,[13] (eqs 3 and 4) and was converted to **I** via a typical hydrosilylation reaction (eq 5) using Speir's catalyst (H_2PtCl_6) made according to literature procedures.[12]

Figure 1 shows the electronic absorption spectra of **I** in comparison to those of MB (from Aldrich) at two different concentrations. In solution, MB molecules tend to associate (forming dimers) due to London–Margenau attractive forces between their π-systems, counterbalanced by electrostatic and Lennard-Jones repulsive forces; the potential energy of association between two identical dye molecules is to a first approximation, proportional to $f^2(\lambda_{max})^3$, where f is the oscillator strength, and both f and λ_{max} refer to the monomer.[15,16] Large values of f and λ_{max} ensure stabilizing association, and that is exactly what is expected of dyes such as MB and **I**. The association between MB ions manifests itself via a blue-shift of the visible absorption spectrum of MB at higher concentrations.[15,16]

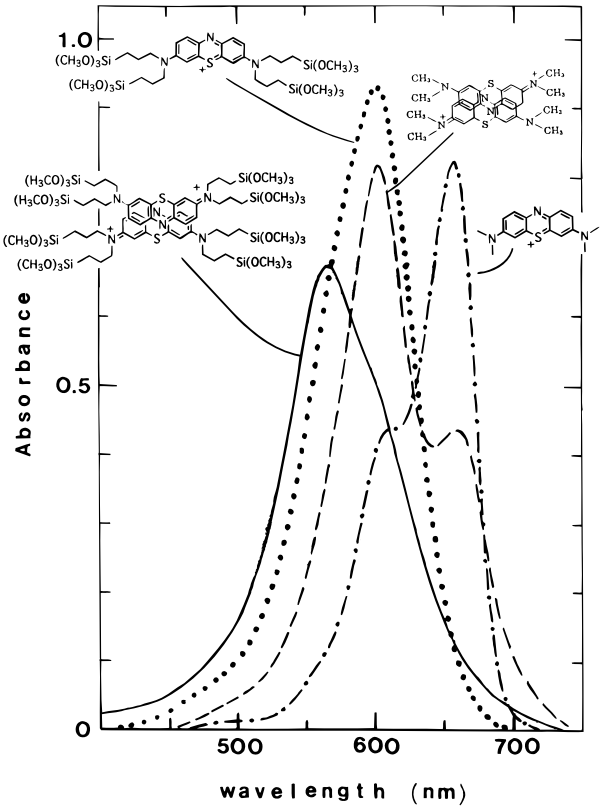

Figure 1. Absorption spectra of **I** in comparison to those of MB in water (*l*: cell length). MB (–·–) (1.13×10^{-5} M, $l = 1$ cm); MB (– – –) (1.13×10^{-3} M, $l = 0.015$ cm); **I** (···) (1.22×10^{-5} M, $l = 1$ cm); **I** (—) (7.64×10^{-4} M, $l = 0.015$ cm). (The possible structure of the dimer of **I** has been drawn in analogy to the corresponding structure suggested for MB.[16])

Therefore, in analogy to MB we attribute the short-wavelength shoulder in the spectrum of **I**, and the blue-shift of λ_{max} at higher concentrations, to dimers (and possibly higher associations) formed from monomers lying flat on top of one another at a distance that should not be very different from 3.12 Å, which is the distance between monomer units calculated by Rabinowich and Epstein for dimers of thionin, another well-known thiazine dye.[15]

Figure 2A shows the electrochemical characterization of **I** in an aqueous, approximately neutral environment. The shape of the reduction wave at potentials more negative than the peak potential (−0.22 V vs Ag/AgCl) indicates a semiinfinite diffusion-limited process, which

(15) (a) Rabinowitch, E.; Epstein, L. F. *J. Am. Chem. Soc.* **1941**, *63*, 69. (b) Mukerjee, P.; Ghosh, A. K. *J. Am. Chem. Soc.* **1970**, *92*, 6403. (c) Mukerjee, P.; Ghosh, A. K. *J. Am. Chem. Soc.* **1970**, *92*, 6419. (d) Kuwabata, S.; Nakamura, J.; Yoneyama, H. *J. Electroanal. Chem. Interfacial Electrochem.* **1989**, *261*, 363.

(16) Bergmann, K.; O'Konski, C. T. *J. Phys. Chem.* **1963**, *67*, 2169.

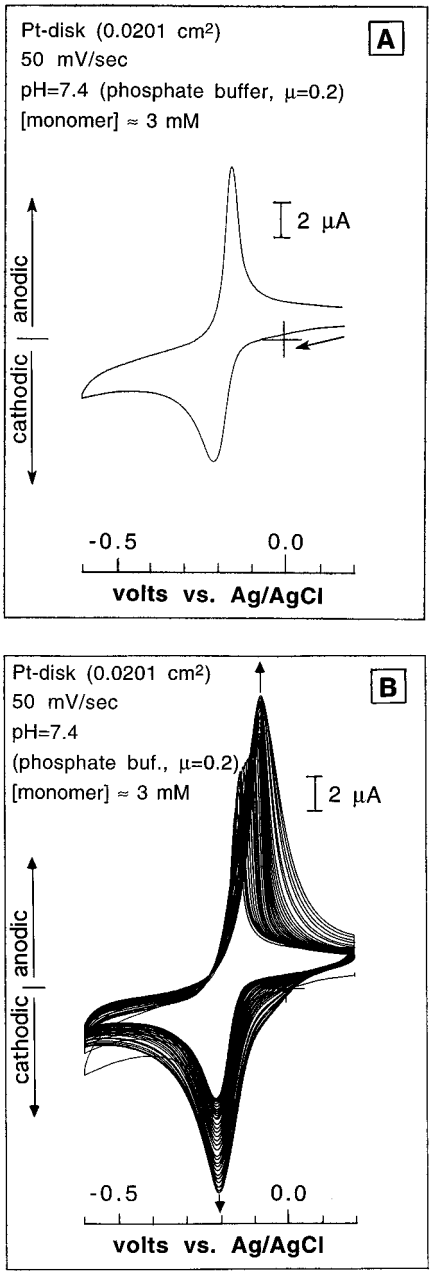

Figure 2. (A) Cyclic voltammetry of **I**. (B) Evolution of the cyclic voltammogram of **I** upon continuous cycling of the potential. CVs were recorded every five scans.

means that the species undergoing reduction (i.e., **I**) is in solution. On the contrary, the return oxidation wave is sharp, indicating a charge-transfer-controlled process, which in turn means that at least part of the species undergoing oxidation (i.e., the reduced form of **I** in analogy to eq 2) is confined on the electrode surface, in agreement to what Svetlicic et al. have reported for MB itself in the same pH range.[10]

Electrochemically Assisted Polymerization of I. If during cyclic voltammetry of **I** the electrode potential is left cycling repetitively (see Figure 2B), the area underneath the cyclic voltammogram increases, indicating accumulation of material on the electrode. Figure 3 shows a photograph of an ITO electrode first patterned photolithographically[14] with strips of nonconducting zones (from which ITO has been removed) and then cycled as shown in Figure 2B. Film curing was accomplished by air-drying at room temperature for 2 days. Clearly, the areas where ITO has been removed (and therefore do not operate as electrodes) have not been derivatized with the blue film. It is well established that an aqueous environment like the one used as the deposition solution promotes stepwise hydrolysis of the $-Si(OCH_3)_3$ groups to $-Si(OH)_3$, which are able to undergo condensation and oligomerization.[1,17] On the other hand, based on the interpretation of the cyclic voltammetric data for **I** (Figure 2A), it is reasonable to suggest that large neutral organic species such as those that would result from reduction (see eq 2) of the hydrolysis product of **I** and oligomers thereof precipitate where they are formed, i.e., on the electrode. A plausible mechanism for film formation then involves reductive precipitation of both hydrolyzed **I** and oligomers formed from **I**, followed by condensation and cross-linking accelerated by the high concentration of the $-Si(OH)_3$ groups in the precipitate.[17,18a] Scheme 2 summarizes the proposed mechanism for film formation, incorporating the electrochemically assisted precipitation step and emphasizing that hydrolysis of $-Si(OCH_3)_3$ groups need not be complete when condensation starts.

Film Characterization. The structure−property relationships of the films were probed spectroscopically and electrochemically.

Infrared and XPS Spectra. The grazing angle IR absorption spectrum of a typical film is shown in Figure 4. The bands at 1224 and 1064 cm^{-1} are assigned to the Si−O−Si asymmetric stretching modes, while the band at 836 cm^{-1} can be assigned to the symmetric Si−O−Si stretching or to vibrational modes of ring structures.[18b] The IR spectrum is rather inconclusive regarding the survival of hydroxyl groups in the films: even though the weak absorption at 992 cm^{-1} could be assigned to Si−OH stretching, the lack of a broad absorption centered at ∼3400 cm^{-1} (that could be assigned to isolated and hydrogen-bonded SiO−H stretching vibrations and hydrogen-bonded water) suggest no quantitative presence of hydroxyl groups in the film. This important issue is related to the degree of cross-linking in the films, and in order to obtain complementary information we turned to XPS (Figure 5). The O:N peak area ratio in the XPS spectrum is 3.3:1, and by considering the atomic sensitivities of O and N (0.63 and 0.38, respectively)[19] it is calculated that the relative atomic ratio of O to N in the film is 2.0:1; hence, we conclude that our drying conditions lead to exhaustive cross-linking of the $-Si(OH)_3$ groups yielding a three-dimensional network with postulated stoichiometry:

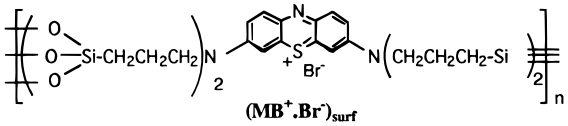

$(MB^+.Br^-)_{surf}$

Electronic Absorption Spectra. The electronic absorption spectrum of $(MB^+ \cdot X^-)_{surf}$ is blue-shifted and broader (Figure 6a) compared with the low-concentration spectrum of **I** (also included as a dashed line in

(17) (a) Arkles, B. *CHEMTECH* **1977**, *7*, 766. (b) Bookbinder, D. C.; Wrighton, M. S. *J. Electrochem. Soc.* **1983**, *130*, 1080. (c) Leventis, N.; Chung, Y. C. *Chem. Mater.* **1992**, *4*, 1415.

(18) Reference 1c: (a) Chapter 10, pp 617−672. (b) pp 541−546. (c) p 506.

(19) *Handbook of X-ray Photoelectron Spectroscopy*; Muilenberg, G. E., Ed.; Perkin-Elmer Corp.: Eden Prairie, MN, 1979; p 188.

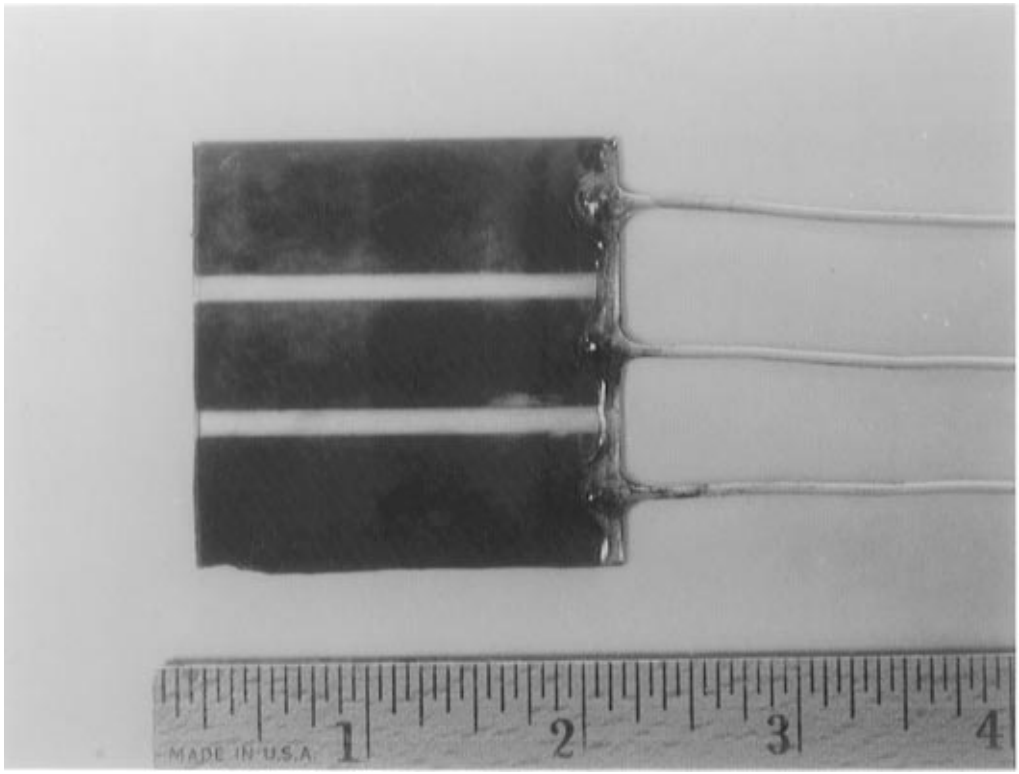

Figure 3. Photograph of a piece of ITO-coated glass, photolithographically patterned[14] with alternating conducting and insulating zones (where ITO has been removed), and derivatized with $(MB^{+}\cdot Br^{-})_{surf}$ (thickness = 1700 Å).

Scheme 2. Mechanism for an ITO-Electrode Surface Derivatization with Films Derived from I

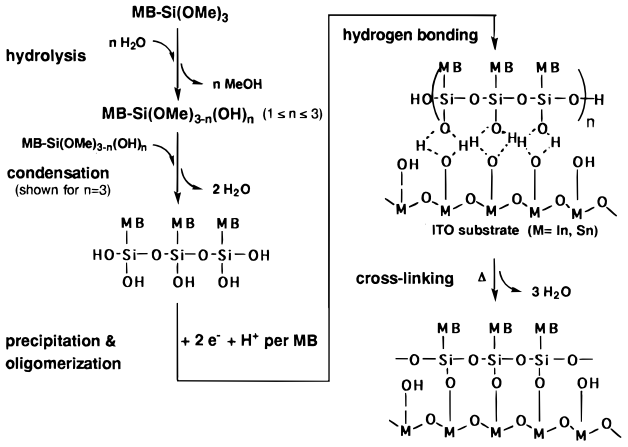

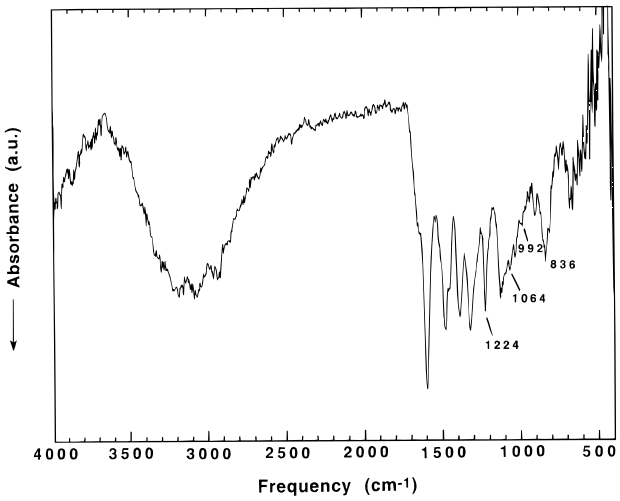

Figure 4. Grazing angle FTIR spectrum of $(MB^{+}\cdot Br^{-})_{surf}$ (thickness = 1500 Å) on a Cr/Au-coated glass slide.

Figure 6 for comparison), implying that chromophores are held close to each other so that their π-systems experience stabilizing interactions qualitatively similar to those responsible for dimer formation in concentrated solutions of the monomer. Upon reduction $(MB^{+}\cdot X^{-})_{surf}$-modified electrodes decolorize while the absorption maximum shifts gradually to longer wavelengths, eventually reaching the maximum absorbance wavelength of **I** at low concentrations (Figure 6e). From that point on, further reduction causes a decrease in intensity but no further red-shift. Since it is expected that two adjacent thiazine moieties in $(MB^{+}\cdot X^{-})_{surf}$ experience the strongest stabilizing interactions when both are oxidized (i.e., when both f and λ_{max} are maximized), Figure 6 suggests that during progressive reduction and once the statistical distribution of the fixed thiazine moieties in the film dictates no neighboring pairs with both members in the oxidized form, the potential energy of stabilization decreases, and the absorption spectrum assumes the features of the monomer. Similar behavior can be observed in spectra of MB-loaded films of Nafion,[15d,20] probably for analogous reasons.

Electrochemical Studies. The redox chemistry of $(MB^{+}\cdot X^{-})_{surf}$ is pH-dependent (Figure 7), but it deviates substantially from that of MB either in solution[11a] or in Nafion.[20,21] Several aspects of the electrochemistry of $(MB^{+}\cdot X^{-})_{surf}$ are summarized in Figure 8.

First, the formal potential, $E^{\circ\prime}$ (measured as halfway between peak maxima from the higher sweep rate traces of Figure 7) depends linearly on the pH at pH < 5.0 with slope approximately equal to −90 mV/pH unit

(20) Guadalupe, A. R.; Liu, K. E.; Abruna, H. D. *Electrochim. Acta* **1991**, *36*, 881.
(21) Lu, Z.; Dong, S. *J. Chem. Soc., Faraday Trans.* **1988**, *84*, 2979.

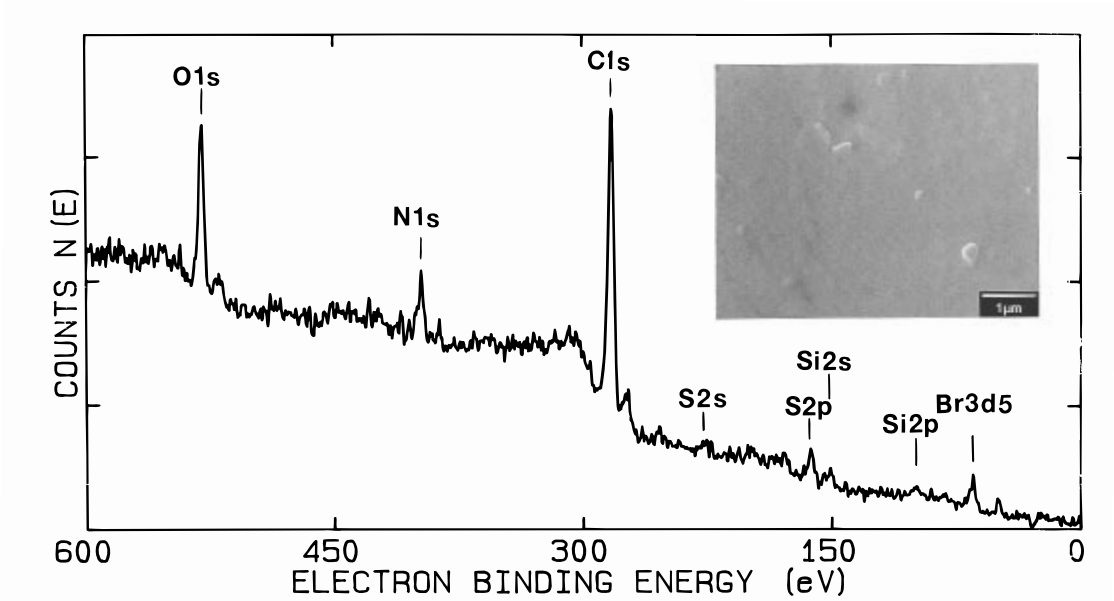

Figure 5. XPS and SEM of $(MB^+ \cdot Br^-)_{surf}$ (thickness = 1500 Å) on a gold foil electrode.

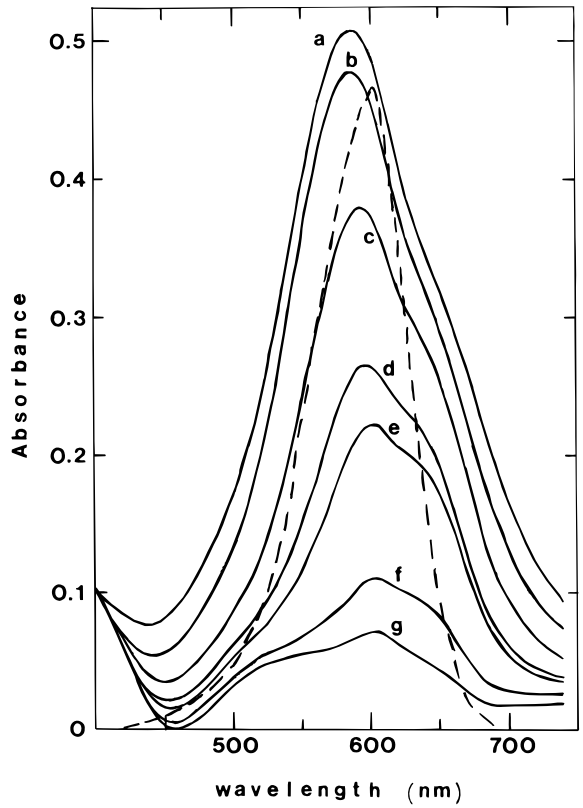

Figure 6. Absorption spectra of $(MB^+ \cdot X^-)_{surf}$ on ITO (1.40 cm^2; $\Gamma = 3.50$ mC/cm^2) in Ar-degassed 0.5 M aq K_2SO_4 solution at pH = 7.0. (a) 0.35 V; (b) −0.05 V; (c) −0.10 V; (d) −0.2 V; (e) −0.3 V; (f) −0.4 V; (g) −0.45 V vs Ag/AgCl. (− − −) Low concentration spectrum of **I** (1.22×10^{-5} M, from Figure 1; for actual absorbance A-scale × 2) included for comparison.

(Figure 8A), meaning that three protons are involved in a two-electron process (eq 6), in analogy to the

$$(MB^+)_{surf} + 2e + 3\ H^+ \rightleftharpoons (H_2LMB^{2+})_{surf} \qquad (6)$$

electrochemistry of MB both in solution and in Nafion films in the same pH range (see eq 1). (H_2LMB^{2+} is the doubly protonated LMB moiety; see eq 1.) At pH ≥ 5.0, $E^{\circ\prime}$ becomes pH-independent, in sharp contrast to the behavior of MB both in solution and in Nafion where the slope is ∼−30 mV/pH unit, indicating a 2e/1 H^+ process according to eq 2. The independence of $E^{\circ\prime}$ from the pH at pH ≥ 5.0 is an unusual phenomenon but not unique, as similar behavior was reported recently for MB entrapped in poly(pyrrole).[22] It is suggested herewith that these phenomena are related to proton availability within the film, and the elucidation of this hypothesis has provided valuable structural and ion percolation information about $(MB^+ \cdot X^-)_{surf}$.

Meanwhile the reduction waves of $(MB^+ \cdot X^-)_{surf}$ lack diffusional tails, and Figure 8B shows a linear dependence of the cathodic peak current, $i_{p,c}$, on the sweep rate, ν. That linear dependence is expected to follow eq 7,[23]

$$i_{p,c} = \frac{n^2F^2}{4RT}\nu A\Gamma \qquad (7)$$

and since the slope at pH = 3.5 (0.08_3 mA s mV^{-1}; $R^2 = 1.0$) is approximately equal to the average of the slopes at pH = 6.8 (0.070 mA s mV^{-1}; $R^2 = 0.997$) and at pH = 9.8 (0.11 mA s mV^{-1}; $R^2 = 0.994$), it is concluded that the same number of electrons ($n = 2$) is involved for the reduction of $(MB^+ \cdot X^-)_{surf}$ at both the pH-dependent and the pH-independent region (see Figure 8A), as all the other parameters of eq 7 remain constant (F, R, T have the usual meaning, A is the electrode area, and Γ is the electrode coverage).[24]

Finally, Figure 8C shows a linear correlation between coverage (by CV at 5 mV/s) and film thickness (by profilometry). Importantly, the different degree of interaction between the thiazine moieties in the two redox states, and the different steric requirements of flat MB and folded LMB notwithstanding, the film thickness is found identical in both redox states, and in both the wet and dry forms. These findings are consistent with a rigid film, whose dense structure is

(22) Gao, Z.; Bobacka, J.; Lewenstan, A.; Ivaska, A. *Synth. Met.* **1994**, *62*, 117.

(23) Bard, A. J.; Faulkner, L. R. *Electrochemical Methods*; Wiley: New York, 1980; p 410, eq 10.7.17.

(24) If for instance only one electron ($n = 1$) was involved in the reduction of $(MB^+ \cdot X^-)_{surf}$ per monomer unit at pH > 5.0, then the slope of $i_{p,c}$ vs scan rate in that pH range should have been 4 times smaller than the slope at pH = 3.5, because $i_{p,c}$ depends on n^2, according to eq 7.

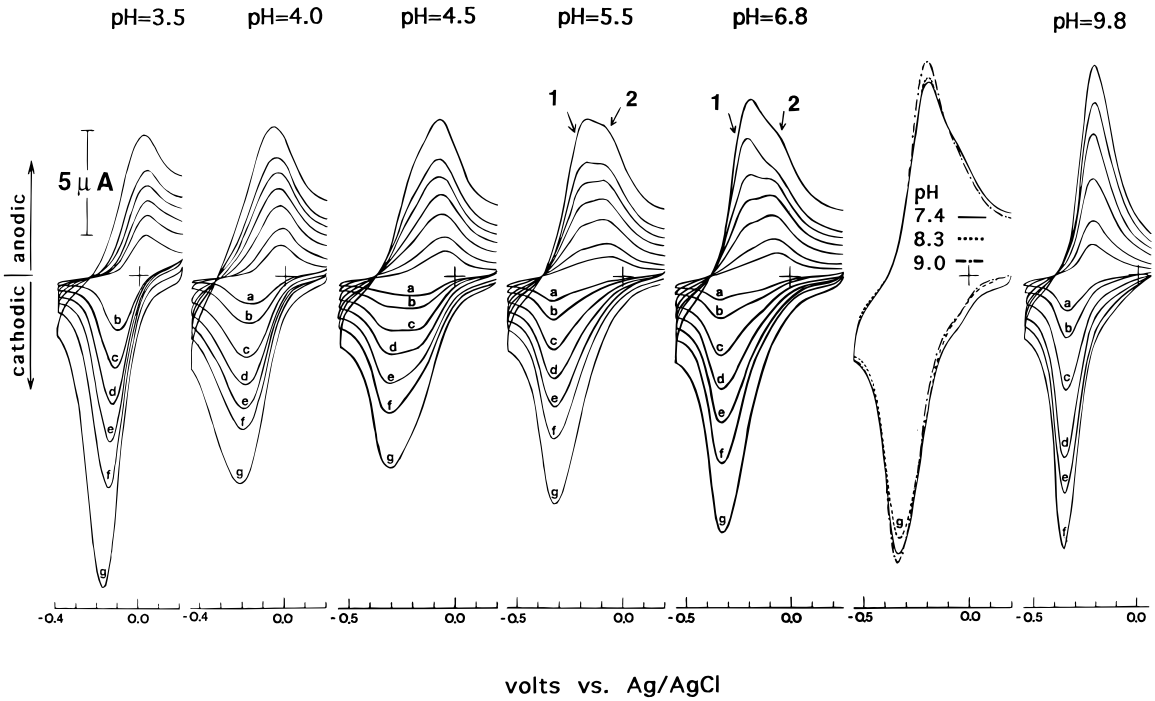

Figure 7. Cyclic voltammetry as a function of pH and sweep rate of a Au disk electrode (0.0201 cm^2) derivatized with $(MB^+ \cdot X^-)_{surf}$ in Ar degassed 0.5 M aq KCl solution. pH was adjusted with HCl or KOH. Sweep rates: (a) 10; (b) 20; (c) 40; (d) 60; (e) 80; (f) 100; (g) 150 mV/s.

determined by a highly cross-linked, glasslike siloxane network. Films appear smooth by SEM at least down to 0.1 μm level (see Figure 5, inset) and cracking has never been observed even at that high magnification level, consistent with the general consensus that sol−gel films thinner that 0.5−1 μm do not crack regardless of the drying conditions,[18c] probably because of the same energy balance reasons cited elsewhere: namely, since the energy that would be invested to extend a crack in very thin films would be greater than the energy gained from relief of the stress via cracking, cracking is unfavorable.[25] The concentration of the thiazine moieties in the film was calculated from the slope of Figure 8C and was found equal to 3.9 M, a value higher than the highest concentration (3.0 M) of any redox substance (viologen) in a polysiloxane film we are aware of.[17b] The density of the film is calculated from the concentration of the thiazine moieties and is found equal to 2.67 g/cm^3 (assuming Br^- as counterions), a value in the density range of typical soda-lime glass.[26] The distance between thiazine moieties, δ, is estimated from the relationship $N_A C_{thiazine} V = 1$. N_A is Avogadro's number, $C_{thiazine}$ = 3.9 M, and V is the average volume of the elementary building block of the film and is equal to (area of mononer unit) × δ.[27a] Molecular modeling (Scheme 3) indicates that isolated monomer units of $(MB^+ \cdot X^-)_{surf}$ prefer to be flat, and occupy an area of 145.59 Å^2; therefore $\delta \geq$ 2.92 Å. That close proximity of the thiazine moieties favors π-system interactions, thus justifying the blue-shift observed in the absorption spectrum of $(MB^+ \cdot X^-)_{surf}$ relative to that of the monomer. To reconcile the fact that despite the apparent close proximity of thiazine moieties, the blue-shift in the electronic absorption spectrum is not as large as that observed for **I** in solution, we are forced to conclude that the relative orientation of the thiazine moieties in the film is not the same as in the concentrated solution of the monomer (Figure 1); instead, the thiazine moieties are close but rather randomly oriented as would be expected from an amorphous material.

In any event, the most striking feature of Figure 7 is the combined effect of the pH and of the scan rate on the shape of the cyclic voltammograms. It is observed that with the exception of a narrow transition range at 4.0 ≤ pH ≤ 4.5, the shape of the reduction waves is independent of the scan rate. On the contrary, the shape of the oxidation waves varies significantly with both the pH and the scan rate; particularly, the scan rate dependence of the oxidation wave in the range 4.5 ≤ pH ≤ 7.4 clearly shows that a more difficult to oxidize species (arrow 2) is formed relatively slowly from the original reduction product which is captured easily at higher scan rates (arrow 1). Indeed, at slow sweep rates (e.g., 10 mV s^{-1}) apparently all the reduction product that corresponds to peak 1 has time to be converted to the species of shoulder 2, so that peak 1 is no longer observed. At higher pH's the shoulder shown by arrow 2 seems to move to more negative potentials, eventually merging completely with the main peak shown by arrow 1. Since all these phenomena are pH-dependent, it is reasonable to attribute them to the proton availability, or lack thereof, within the films: as pH increases, proton flux into the film is expected to be slower because of the smaller chemical potential gradient of protons between the film and the electrolyte. Furthermore, proton transfer between sterically hindered amines is known to be slow,[28] and if that is extrapolated into the case of $(MB^+ \cdot X^-)_{surf}$, it points toward the dense film structure, and toward the fixed cationic sites which

(25) Lange, F. F. In *Fracture Mechanics of Ceramics, Microstructure Materials and Applications*; Bratt, R. C., Hasselman, D. P. H., Lange, F. F., Eds.; Plenum Press: New York, 1974; Vol. 2, pp 599−609.

(26) Sawyer, D. T.; Sobkowiak, A.; Roberts, J. L. *Electrochemistry for Chemists*, 2nd ed.; Wiley: New York, 1995; p 226.

(27) *Electroactive Polymer Electrochemistry: Part 1 Fundamentals*; Lyons, M. E. G., Ed.; Plenum Press: New York, 1994: (a) p 11, eq 18; (b) p 140; (c) p 125, eqs 258 and 260; (d) pp 9−10 and references therein.

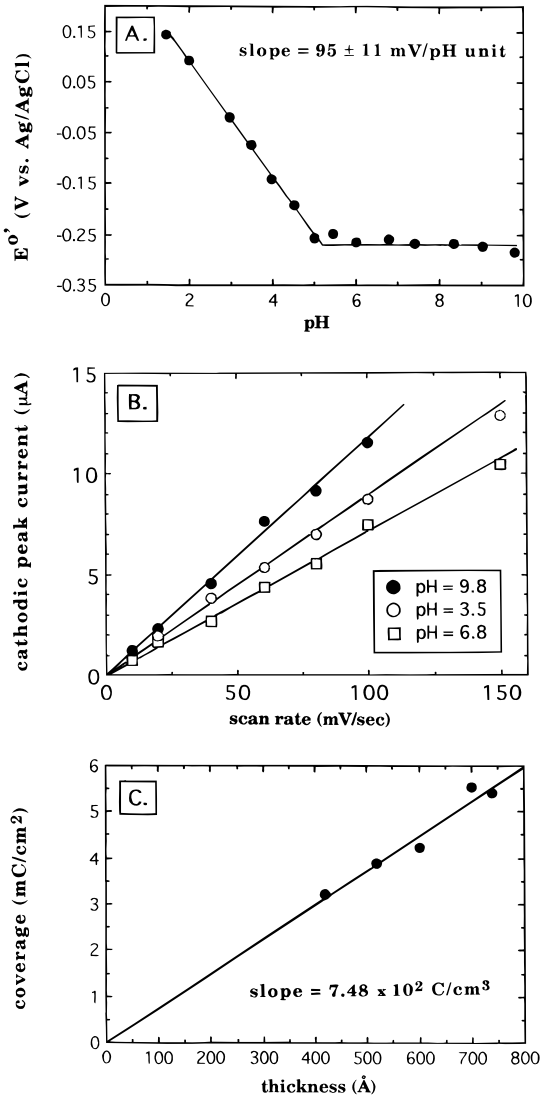

Figure 8. (A) $E^{o\prime}$ of $(MB^{+}\cdot X^{-})_{surf}$ as a function of pH. (Data from Figure 7.) (B) Sweep rate dependence of the cathodic peak current at three pHs. (Data from Figure 7.) (C) Coverage, Γ (by CV), as a function of film thickness (by profilometry) of $(MB^{+}\cdot X^{-})_{surf}$ on Cr/Pt sputtered glass slide electrodes [phenothiazine moieties] = slope/nF = 3.9 M (n = 2).

Scheme 3. Structural Energy Minimized Three-Dimensional Model of the Monomer Unit of $(MB^{+}\cdot X^{-})_{surf}$

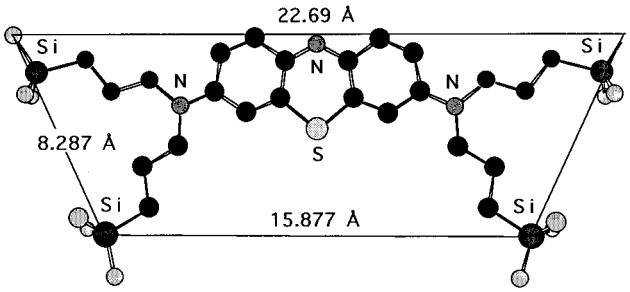

retard transport of protons even further.[29] Eventually, at pH = 9.8 the shape of the CV does not depend on the scan rate, since no protons penetrate into the film during the time scale of cyclic voltammetry.

If the poor proton-availability hypothesis employed in order to explain the pH and sweep rate dependence

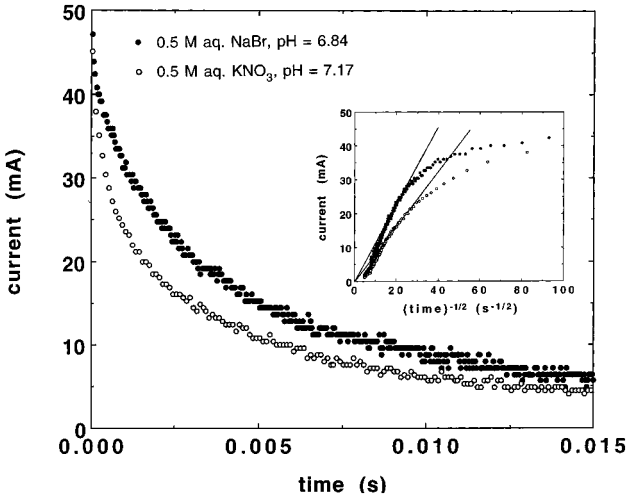

Figure 9. Typical chronoamperometric data using a Cr/Au-coated glass slide as an electrode (0.618 cm²) derivatized with $(MB^{+}\cdot X^{-})_{surf}$ (Γ = 3.7 mC/cm²) and stepped from 0.35 to −0.5 V vs Ag/AgCl in different electrolytes. Inset: plot of the current vs (time)$^{-1/2}$ for calculation of the apparent diffusion coefficients of charge transport in $(MB^{+}\cdot X^{-})_{surf}$. Deviations from linearity (i.e., from Cottrell behavior) at short times after the potential step are usually attributed to the film's uncompensated resistance, while deviations at longer times are due to the finite nature of the film.[27b]

of the cyclic voltammograms is correct, we should expect that after a two-electron reduction in the pH-independent region, the charge electroneutrality of the films will be maintained by an influx of the most available cations. Support for this argument is provided by the ionic dependence of the apparent diffusion coefficient of charge transport, D_{CT}. At short times (<2 ms) after a large-amplitude potential step in the negative direction (see for example Figure 9), films of $(MB^{+}\cdot X^{-})_{surf}$ demonstrate a Cottrell-type response (see Figure 9, inset), allowing calculation of D_{CT} from the slope of the cathodic current vs (time)$^{-1/2}$, via eq 8.[27c] Results for

$$\text{at short times:} \qquad i(t) = \frac{nFAD_{CT}^{1/2}C_{thiazine}}{\pi^{1/2}t^{1/2}} \qquad (8)$$

various 1:1 electrolytes at pH = 7.0 and 9.5 are summarized in Table 1. At first glance the D_{CT} values are surprisingly low given the close proximity of redox sites in the film;[30] this fact, however, is reconciled easily by considering a restricted transport of charge-compensating ions due to a dense film structure. Indeed, Table 1 and Figure 10 show that the D_{CT} values are sensitive to the chemical identity of both the cation and the anion, a behavior which is different from that of MB in Nafion where reportedly reduction depends only on the anion.[21] Furthemore, the D_{CT} for the same supporting electrolyte are equal (within experimental error) at pH = 7.0 and pH = 9.5 (i.e., within the pH-independent range). This observation is consistent with the model we are introducing for the redox chemistry of the $(MB^{+}\cdot X^{-})_{surf}$ films at pH > 5.0, namely, that the

(28) Meot-Ner (Mautner), M.; Smith, S. C. *J. Am. Chem. Soc.* **1991**, *113*, 862.

(29) (a) Denisevich, P.; Willman, K. W.; Murray, R. W. *J. Am. Chem. Soc.* **1981**, *103*, 4727. (b) Ikeda, T.; Schmehl, R.; Denisevich, P.; Willman, K. W.; Murray, R. W. *J. Am. Chem. Soc.* **1982**, *104*, 2683. (c) Burgmayer, P.; Murray, R. W. *J. Phys. Chem.* **1984**, *88*, 2515.

(30) The D_{CT} values for $(MB^{+}\cdot X^{-})_{surf}$ are at least 1 order of magnitude lower than values for analogous siloxane films incorporating viologen (0.4−3 × 10^{-10} cm² s^{-1}).[17b]

Table 1. Apparent Diffusion Coefficients of Charge Transport in $(MB^+\cdot X^-)_{surf}$,[a] Measured by Chronoamperometry in 0.5 M Aqueous Solutions of the Corresponding Electrolytes at Two Different pHs[b]

cation	K^+		Na^+		Li^+		Bu_4N^+	
Stokes radius (Å)[31]	1.25		1.83		2.37		4.71	
pH	7.0	9.5	7.0	9.5	7.0	9.5	7.0	9.5
F^-	$7._1 \pm 1.1$	$7._8 \pm 1.2$	$7._6 \pm 0.4$	$6._5 \pm 1.7$				
Cl^-	$16._1 \pm 2.5$	$15._7 \pm 1.7$	$11._3 \pm 1.0$	$13._3 \pm 1.0$	$8._0 \pm 0.9$	$8._7 \pm 0.9$	$2._9 \pm 0.6$	
(in D_2O)			$(5._4 \pm 1.0)$					
NO_3^-	$15._3 \pm 1.6$	$15._6 \pm 2.0$	$18._2 \pm 3.5$	$16._5 \pm 2.7$	$7._5 \pm 1.3$	$8._3 \pm 0.4$		
(in D_2O)	$(4._3 \pm 1.1)$		$(4._0 \pm 1.5)$					
Br^-	$23._8 \pm 3.0$	$19._8 \pm 3.2$	$19._8 \pm 2.2$	$21._0 \pm 3.5$	$9._0 \pm 2.1$	$8._0 \pm 1.4$	$3._4 \pm 0.9$	$3._4 \pm 1.1$
ClO_4^-			$5._4 \pm 2.0$	$4._9 \pm 2.0$	$4._8 \pm 1.8$	$4._2 \pm 1.8$		
I^-	$11._6 \pm 3.1$	$12._0 \pm 4.5$	$3._9 \pm 1.1$	$3._5 \pm 1.9$	$2._0 \pm 0.4$			

[a] In $cm^2\ s^{-1} \times 10^{12}$. [b] For 95% confidence limits multiply the standard deviations by a factor of 2; average of three Au and three Pt electrodes, each stepped twice.

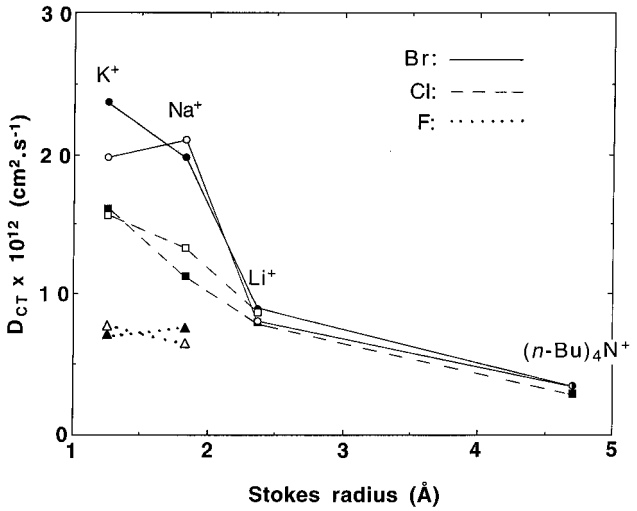

Figure 10. Plot of the diffusion coefficients of charge transport of $(MB^+\cdot X^-)_{surf}$ for selected electrolytes as a function of pH and the Stokes radius of the cation (data from Table 1). (●, ■, ▲) pH = 7.0; (○, □, △) pH = 9.5.

primary reduction process does not involve protons, but cations from the supporting electrolyte instead. Additionally, substitution of H_2O with D_2O in selected experiments (see Table 1) results in significantly lower D_{CT} values suggesting that movement of ions is accompanied by movement of water or perhaps that charge compensating ions are hydrated. That leads to another observation, namely that D_{CT}s are sensitive to the Stokes radius of the cation of the supporting electrolyte (see Figure 10),[31] dropping significantly for the larger cations Li^+ and Bu_4N^+; this sensitivity can be taken as further evidence that charge compensation upon reduction is brought about by an influx of the cations of the electrolyte. Significantly, while cations are entering the film, electroneutrality dictates that anions must be leaving the film. However, the departure of anions must be also restricted, as can be judged by the fact that the D_{CT} values for K^+ or Na^+ electrolytes change significantly with the nature of the anion. These results indicate that probably the pore sizes in the films are less than twice the Stokes radius of Na^+, or that the pore size distribution in the siloxane network is centered in the range between 3 and 4.0 Å, which is in excellent agreement with the distance between thiazine moieties calculated from the concentration data above.

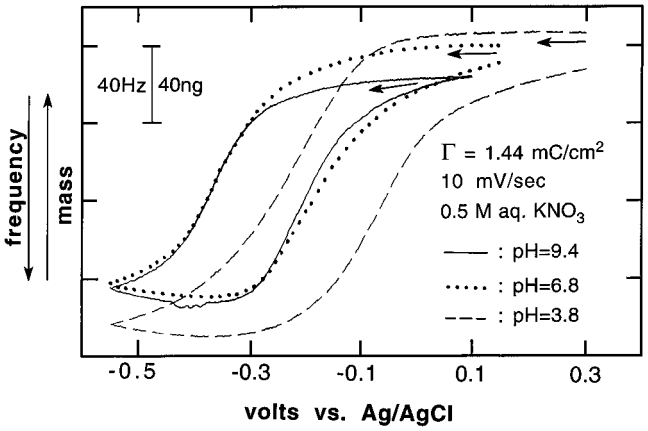

Figure 11. Quartz crystal microbalance (QCM) results for $(MB^+\cdot X^-)_{surf}$ on a Au electrode (0.2 cm^2) at three different pHs.

At this point, the early stages of the redox chemistry of $(MB^+\cdot X^-)_{surf}$ in the pH-independent region may be summarized in eq 9:

$$(MB^+\cdot X^-)_{surf} + 2e + M^+_{solution} \rightleftharpoons (MB^-\cdot M^+)_{surf} + X^-_{solution} \quad (9)$$

However, if we are allowed to draw conclusions by analogy to the electrochemistry of MB in solution (eq 2), the fixed anionic moieties in $(MB^-\cdot M^+)_{surf}$ are not expected to be thermodynamically stable and should undergo protonation to the neutral leuco forms (LMB) according to eq 10:

$$(MB^-\cdot M^+)_{surf} + H^+_{solution} \rightleftharpoons LMB_{surf} + M^+_{solution} \quad (10)$$

Supporting evidence for the relative involvement of cations vs protons in the time scale of the cyclic voltammetry is obtained by monitoring the mass of $(MB^+\cdot X^-)_{surf}$ films during cyclic voltammetry at various pH's using a quartz crystal microbalance (Figure 11).[32] The basic assumption and justification of that experiment was that any mass changes observed during cyclic voltammetry should be traceable to the balance between the cations and anions entering or leaving the film. According to Figure 11, upon reduction, $(MB^+\cdot X^-)_{surf}$ films loose mass at all pH's; at higher pH's (~9.8) that loss is minimal because according to eq 9 hydrated anions are replaced by hydrated cations from the supporting electrolyte which are heavier than protons;

(31) (a) Robinson, R. A.; Stokes, R. H. *Electrolyte Solutions*; Butterworth: London, 1959; pp 125−126. (b) Crumbliss, A. L.; Lugg, P. S.; Morosoff, N. *Inorg. Chem.* **1984**, *23*, 4701.

(32) Buttry, D. A.; Ward, M. D. *Chem. Rev. (Washington, D.C.)* **1992**, *92*, 1355.

at intermediate pH's (~7.0) films lose more mass, implying that anions are replaced by both cations and protons as the effect of both eqs 9 and 10 would become significant for the thickness of the particular film within the period of the cyclic potential sweep. Finally, to reconcile the mass loss upon reduction in the pH-dependent range (e.g., pH = 3.8) with the fact that reduced phenothiazine moieties must end up doubly protonated according to eq 6 thus requiring more charge-compensating anions in the films, we are forced to assume a source of anions within the films in analogy to what has been suggested for films of poly(thionin) in strongly acidic media.[33] Therefore, at low pH's (<5.0) films may lose mass upon reduction *only if* the protons required by eq 6 originate from within the film, which in turn might imply that the phenothiazine moieties are protonated. Consequently, films loose more mass at pH ~ 3.8 because of the larger mass difference between retained protons and departing anions.

Thermodynamics provide the driving force, but it is improbable that simple hydrodynamic flow is able to support the proton flux required in order for eq 10 to have an effect on the position and shape of the cyclic voltammetric waves at pH > 5.0. One reason for this is that the diffusion coefficient of protons in $\mathbf{(MB^+\cdot X^-)_{surf}}$ should be very small: even though polysiloxane networks carrying the fixed cationic sites of one-electron reduced viologen moieties are less dense than $\mathbf{(MB^+\cdot X^-)_{surf}}$, nevertheless the diffusion coefficient of protons through those viologen films was estimated at about 1.3×10^{-12} cm^2 s^{-1},[34] a value already significantly lower than most D_{CT}s of Table 1. Furthermore, if hydrodynamic flow alone had provided the protons needed for the reduction of $\mathbf{(MB^+\cdot X^-)_{surf}}$ from the outset, no phenomena associated with the flux of cations would have been observed, and the redox chemistry would have been analogous to the one in solution at pH > 6.0. Finally, the scan rate independence of the reduction wave shape and position at pH > 5.0 is consistent with a low proton availability within the oxidized films, and reinforces the need for a mechanism that enhances the proton flux upon reduction in order to explain the strong dependence of the shape of the oxidation waves on the scan rate. Such a plausible mechanism involves proton exchange (hopping) between unprotonated, $\mathbf{MB^-_{surf}}$, and protonated, $\mathbf{LMB_{surf}}$, sites according to eq 11:[35]

$$MB^-_{surf}(i) + LMB_{surf}(i+1) \underset{k_H}{\overset{k_H}{\rightleftharpoons}} LMB_{surf}(i) + MB^-_{surf}(i+1) \quad (11)$$

(i and i+1 refer to adjacent sites in the polysiloxane network, and k_H is the bimolecular rate constant of the proton exchange.) It is not difficult to prove in analogy to other work[27d] that this proton-transfer process can be described by a Fickian flux, $J_{H^+,hop}$, which in one dimension can be stated as

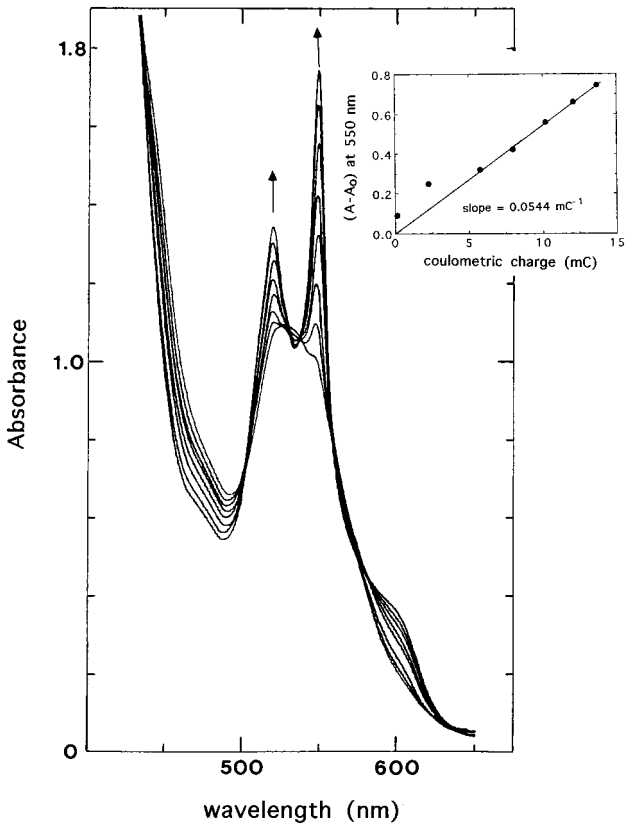

Figure 12. Coulometric titration of cytochrome c (1×10^{-4} M in Ar degassed 1 M aq $NaClO_4$ at pH = 7.0) with a gold electrode (4.75 cm^2) derivatized with $\mathbf{(MB^+\cdot X^-)_{surf}}$ ($\Gamma = 4.48$ mC cm^{-2}), stepped from 0.35 V vs Ag/AgCl to −0.35 V vs Ag/AgCl and held at −0.35 V vs Ag/AgCl for 42 min under continuous Ar purge. The quasi-steady-state current density was 4.2 μA cm^{-2}. The total amount of the reduced form of cytochrome c produced was 6.77×10^{-5} mmol corresponding to 39% conversion of the oxidized form. Inset: The slope is equal to $(\epsilon_{red} - \epsilon_{ox}) \times \alpha/(nFV)$, where α is the current efficiency, V is the volume of the cytochrome c solution (1.75 mL), and at 530 nm the difference of the extinction coefficients $(\epsilon_{red} - \epsilon_{ox}) = 19\,280$ cm^{-1} M^{-1}.[37] It is calculated that $\alpha = 0.48$.

$$J_{H^+,hop} = D_{H^+,hop}(\partial[MB^-_{surf}]/\partial x) = -D_{H^+,hop}(\partial[LMB_{surf}]/\partial x) \quad (12)$$

with the diffusion coefficient given by

$$D_{H^+,hop} = k_H \delta^2 [MB^-_{surf} + LMB_{surf}] \quad (13)$$

(The actual derivation of eq 12 is given in the Appendix). In the oxidized films, the bracketed quantities in eq 13 vanish, and therefore the proton-exchange mechanism is not operative, resulting in a pH-independent reduction wave.

Applications of $\mathbf{(MB^+\cdot X^-)_{surf}}$. Films of $\mathbf{(MB^+\cdot X^-)_{surf}}$ retain the electrochromic properties of methylene blue as was demonstrated in Figure 6 and therefore are appropriate for application in electrochromic devices. Furthermore, films of $\mathbf{(MB^+\cdot X^-)_{surf}}$ retain the electrocatalytic properties of methylene blue as well. For example it is known that cytochrome c is electroinactive at potentials close to its standard electrochemical potential on gold or platinum electrodes.[36] Figure 12 demonstrates spectrophotometrically that gold foil elec-

(33) Hillman, A. R.; Loveday, D. C.; Swann, M. J.; Eales, R. M.; Hammett, A.; Higgins, S. J.; Bruckenstein, S.; Wilde, C. P. *Faraday Discuss. Chem. Soc.* **1989**, *88*, 151.

(34) Leventis, N.; Chung, Y. C. *J. Mater. Chem.* **1993**, *3*, 833.

(35) (a) Glasstone, S.; Laidler, K. J.; Eyring, H. *The Theory of Rate Processes*; McGraw-Hill: New York, 1941; Chapter X. (b) Ruff, I.; Botar, L. *J. Chem. Phys.* **1985**, *83*, 1292. (c) Botar, L.; Ruff, I. *Chem. Phys. Lett.* **1986**, *126*, 348.

(36) (a) Eddowes, M. J.; Hill, H. A. O. *J. Am. Chem. Soc.* **1979**, *101*, 4461. (b) Yeh, P.; Kuwana, T. *Chem. Lett.* **1977**, 1145.

trodes coated with $(\mathbf{MB^{+}\cdot X^{-}})_{\mathbf{surf}}$ are able to mediate the reduction of cytochrome *c* in analogy to films incorporating viologen.[37] The current efficiency was calculated at ~50%, with the most probable side reactions being hydrogen evolution and the initial reduction of the $(\mathbf{MB^{+}\cdot X^{-}})_{\mathbf{surf}}$ film.

Conclusions

Polysiloxane networks incorporating covalently bonded redox dyes can be formed by an electrochemically assisted sol−gel process, via manipulation of the solubility of trimethoxysilyl-group-modified monomers. This premise was demonstrated with a thiazine dye (**I**) analogous to methylene blue. Films derived from **I** are dense holding the dye moieties in close proximity (ca. 3−4 Å) thus forcing π-system interactions that are reflected in the absorption spectra. The resulting narrow channels between thiazine moieties restrict the ionic transport that maintains electroneutrality during redox cycling, and therefore the rate of redox switching depends on the size of the ions of the electrolyte. We do not envision any difficulties in generalizing this approach to electrode surface modification with other redox-active dyes. Further work in progress involves dopping sol−gel-derived monoliths with **I**, which due to its $-Si(OCH_3)_3$ groups is expected to develop covalent anchors with the polysiloxane network.

Appendix

Derivation of Eqs 12 and 13. It is postulated that a significant mechanism of proton transport in films of $(\mathbf{MB^{+}\cdot X^{-}})_{\mathbf{surf}}$ involves site-hopping and is based on a degenerate proton-exchange bimolecular reaction between adjacent sites according to eq 11. That mechanism is illustrated in Scheme 4, which also shows the sequence of events during a three-site proton-transport process upon reduction, and the associated flux vectors. For brevity, B_i represents a fixed anionic site of $\mathbf{MB^{-}_{surf}}$, and BH_i represents a fixed protonated (neutral) $\mathbf{LMB_{surf}}$ site, both at position *i*.

The proton exchange reaction of Scheme 4 can be written as

$$BH_i + B_{i+1} \underset{k_H}{\overset{k_H}{\rightleftharpoons}} B_i + BH_{i+1} \qquad (14)$$

The net proton flux is therefore given by

$$J_{H^+,hop} = \underbrace{k_H\delta[BH]_i[B]_{i+1}}_{\text{flux to the right}} - \underbrace{k_H\delta[B]_i[BH]_{i+1}}_{\text{flux to the left}} \qquad (15)$$

But

$$[BH]_{i+1} = [BH]_i + \delta(\partial[BH]/\partial x)_i \qquad (16)$$

$$[B]_{i+1} = [B]_i + \delta(\partial[B]/\partial x)_i \qquad (17)$$

Equation 15 due to eqs 16 and 17 becomes

(37) Lewis, N. S.; Wrighton, M. S. *Science* **1981**, *211*, 944.

Scheme 4

(a) Site-hopping proton transport mechanism

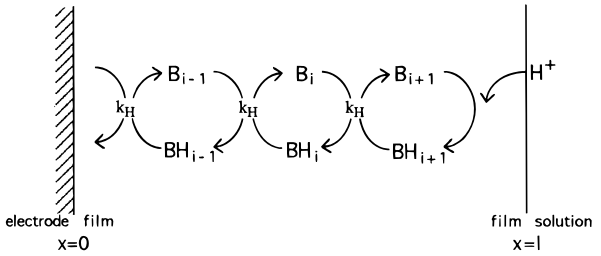

(b) A three-site proton transport sequence of events upon reduction

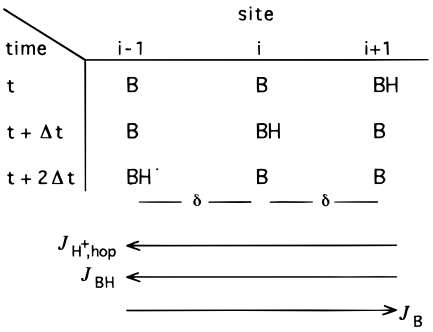

$$J_{H^+,hop} = k_H\delta^2[BH]_i(\partial[B]/\partial x)_i - k_H\delta^2[B]_i(\partial[BH]/\partial x)_i \qquad (18)$$

From Scheme 4 it is obvious that

$$(\partial[BH]/\partial x)_i = -(\partial[B]/\partial x)_i \qquad (19)$$

Therefore eq 18 due to eq 19 becomes

$$J_{H^+,hop} = k_H\delta^2([B] + [BH])_i(\partial[B]/\partial x)_i = -k_H\delta^2([B] + [BH])_i(\partial[BH]/\partial x)_i \qquad (20)$$

And since it was defined that $B = \mathbf{MB^{-}_{surf}}$ and $BH = \mathbf{LMB_{surf}}$ for all *i*, eq 20 can be written as

$$J_{H^+,hop} = D_{H^+,hop}(\partial[MB^{-}{}_{surf}]/\partial x) = -D_{H^+,hop}(\partial[LMB_{surf}]/\partial x) \qquad (12)$$

where

$$D_{H^+,hop} = k_H\delta^2[MB^{-}{}_{surf} + LMB_{surf}] \qquad (13)$$

Acknowledgment. We gratefully acknowledge support from the Air Force Office of Scientific Research (Grant F496-20-94-1-0449), from The Petroleum Research Fund, administered by the ACS (Grant 30396-G7), and from the University of Missouri Research Board. M.C. thanks C. Sotiriou-Leventis for assistance with synthesis and J. A. Switzer and E. Bohannan for assistance with the QCM experiments.

CM970261G